Published in final edited form as:

Neuroscience. 2019 December 01; 422: 146–160. doi:10.1016/j.neuroscience.2019.09.027.

Increased Type I and Decreased Type II Hair Cells after Deletion of *Sox2* in the Developing Mouse Utricle

Jingrong Lu[a,b,c,1], **Lingxiang Hu**[b,c,d,1], **Bin Ye**[a,b,c], **Haixia Hu**[a,b,c], **Yong Tao**[b,c,d], **Yilai Shu**[e,f], **Hao Chiang**[g,h], **Vikrant Borse**[g,h], **Mingliang Xiang**[a,b,c], **Hao Wu**[b,c,d,*], **Albert S. B. Edge**[g,h], **Fuxin Shi**[b,i,*]

[a]Department of Otolaryngology-Head & Neck Surgery, Xinhua Hospital, Shanghai Jiaotong University School of Medicine, Shanghai 200092, China

[b]Ear Institute, Shanghai Jiaotong University School of Medicine, Shanghai 200092, China

[c]Shanghai Key Laboratory of Translational Medicine on Ear and Nose Diseases, China

[d]Department of Otolaryngology Head & Neck Surgery, Shanghai 9th People's Hospital/Shanghai Ninth People's Hospital, Shanghai Jiaotong University School of Medicine, Shanghai 200092, China

[e]ENT Institute and Otorhinolaryngology Department, Affiliated Eye and ENT Hospital, State Key Laboratory of Medical Neurobiology, Fudan University, Shanghai, China

[f]Key Laboratory of Hearing Medicine of National Health and Family Planning Commission (NHFPC), Shanghai, China

[g]Department of Otolaryngology, Harvard Medical School, Boston, MA 02115, USA

[h]Eaton-Peabody Laboratory, Massachusetts Eye and Ear, Boston, MA 02114, USA

[i]Decibel Therapeutics, Boston, MA 02215, USA

Abstract

The vestibular system of the inner ear contains Type I and Type II hair cells (HCs) generated from sensory progenitor cells; however, little is known about how the HC subtypes are formed. *Sox2* (encoding SRY-box 2) is expressed in Type II, but not in Type I, HCs. The present study aimed to investigate the role of SOX2 in cell fate determination in Type I *vs*. Type II HCs. First,

*Corresponding authors. Address: Ear Institute, Shanghai Jiaotong University School of Medicine, 1665 Kongjiang Road, Shanghai 200092, China. wuhao622@sina.cn (H. Wu), fshi@decibeltx.com (F. Shi).

[1]These authors contributed equally to this work.

AUTHOR CONTRIBUTIONS

FS and HW conceived the project; JL FS and AE wrote the manuscript. HW, JL, and LX designed the experiments; YT, YS, and MX provided technical and platform support. JL, LX, and HC participated in manuscript preparation and performed most of the experiments; JL, BY, HC, VB, and HH generated the *Sox2*$^{flox/flox}$; *Gfi1-Cre* mice under the instruction of FS. All authors listed have made substantial and direct contributions to the work, and approved it for publication.

AVAILABILITY OF DATA AND MATERIALS

All data generated or analyzed during this study are included in the published article.

CONSENT FOR PUBLICATION

All authors consent for the publication of this study.

DECLARATIONS OF INTEREST

AE is a founder and consultant to Decibel Therapeutics.

we confirmed that Type I HCs developed from *Sox2*-expressing cells through lineage tracing of *Sox2*-positive cells using a *CAG-tdTomato* reporter mouse crossed with a *Sox2-CreER* mouse. Then, *Sox2* loss of function was induced in HCs, using $Sox2^{flox}$ transgenic mice crossed with a *Gfi1-Cre* driver mouse. Knockout of *Sox2* in HCs increased the number of Type I HCs and decreased the number of Type II HCs, while the total number of HCs and *Sox2*-positive supporting cells did not change. In addition, the effect of *Sox2*-knockout persisted into adulthood, resulting in an increased number of Type I HCs. These results demonstrate that SOX2 plays a critical role in the determination of Type II *vs*. Type I HC fate. The results suggested that *Sox2* is a potential target for generating Type I HCs, which may be important for regenerative strategies for balance disorders.

Keywords

utricle; hair cell; vestibule; SOX2; balance disorder

INTRODUCTION

Hair cells (HCs) of the vestibular system of the inner ear detect head movement and linear acceleration. The saccular and utricular maculae contain Type I and Type II HCs that differ in their location, molecular signature, morphology, and innervation (Eatock and Songer, 2011). Type I HCs are innervated by afferent nerve endings in a calyx complex and express a Ca^{2+} -binding protein, oncomodulin, in the central zone of the maculae (Kevetter and Leonard, 2002; Simmons et al., 2010; Hoffman et al., 2018). Type II HCs form synapses with bouton-type afferent terminals (Yamashita and Ohmori, 1990; Holt et al., 2006). The afferent bouton endings receive signals from 1 to 2 ribbons (Lysakowski and Goldberg, 1997). The macula has two topographical regions: A central striola harboring calretinin+ calyces and a surrounding lateral extrastriola. The striolar region encodes large and fast signals, whereas the extrastriola conducts slow and tonic signals. HCs are patterned along a line of polarity reversal; their stereocilia reverses the orientation to detect linear acceleration in opposing directions. Type I and Type II HCs are found in both striolar and extrastriolar regions. In the rodent striolar region, Type I HCs outnumber Type II HCs by a 3:2 ratio, and in the extrastriolar region, they occur in a ratio of approximately 1:1 (Desai et al., 2005). Accumulating evidence suggests that Type I HCs are more sensitive to detect fast head movement, reflecting their stiffer hair bundles, larger transduction currents, and low input resistance (Li et al., 2010; Contini et al., 2012); Type I HCs conduct nerve impulses faster in the central region than in the peripheral regions, possibly reflecting the higher abundance of presynaptic ribbons (Kirk et al., 2017).

The vestibular organs first develop immature hair bundles at embryonic day (E) 13.5 (Mbiene et al., 1984; Denman-Johnson and Forge, 1999). Half of the HCs develop from progenitors before birth and the remainder develop from supporting cells in the first postnatal week; a small number of HCs continue to be added to the utricle throughout life (Burns et al., 2012). The new HCs express transcription factors of atonal BHLH transcription factor 1 (ATOH1), and then POU class 4 homeobox 3 (POU4F3). Type I HCs arise in a narrow band in the central zone, or striola, of the developing utricular macula

at E14 (Sans and Chat, 1982), and they begin to express oncomodulin at E18 (Simmons et al., 2010). The dynamics of the genesis and lineages of Type I and Type II HCs have not been elucidated. In addition to their structural and homeostatic functions, supporting cells facilitate HC patterning and polarity formation during development, promote HC survival, eliminate dead HCs, and serve as progenitors for new HCs during regeneration (Monzack and Cunningham, 2013; Wan et al., 2013; Burns and Stone, 2017).

SRY-box 2 (SOX2) has roles in cellular reprogramming and stem cell pluripotency. It acts as a transcriptional repressor by binding to a large number of genes and their regulatory regions (Boyer et al., 2005). SOX2 is expressed throughout the developing nervous system and maintains neural progenitor cell fate. SOX2 is required for the formation of the prosensory domain during early otic induction (Kiernan et al., 2005). SOX2 is abundant in the oticplacodes (Kiernan et al., 2005; Dabdoub et al., 2008) and is a marker for the prosensory domain from which the cochlear and vestibular epithelia develop (Kiernan et al., 2005; Hume et al., 2007). However, after birth, it ceases to be expressed in HCs in the auditory system, while being maintained in supporting cells (Hume et al., 2007; Oesterle et al., 2008). Interestingly, *Sox2* expression is downregulated in Type I HCs in the early postnatal period, whereas *Sox2* expression in Type II HCs of the vestibular system is maintained throughout adulthood (Hume et al., 2007; Oesterle et al., 2008). In addition to the expression of *Sox2*, Type I and II HCs can be distinguished by their calcium binding proteins. However, the functional role of SOX2 in Type II HCs has not been determined.

HC formation from progenitors is becoming increasingly well characterized; however, little is known about the differences in signaling pathways that lead to HC subtypes. In the present study, we hypothesized that *Sox2* knockout would favor the genesis of Type I HCs at the cost of Type II HCs. Using a cell-specific knockout approach, we eliminated *Sox2* expression in Type II HCs and found that *Sox2* knockout elicited the generation of Type I IHCs (Fig. 1). Type I HCs were characterized by the expression of a set of markers and calyx formation. This suggested a role of SOX2 in determining the fate of HCs. The observed increase in the number of Type I HCs was maintained until adulthood.

EXPERIMENTAL PROCEDURES

Animals

Sox2^{flox} mice (Shaham et al., 2009) with locus of X-over P1 (loxP) sites flanking the coding exon of *Sox2* in both alleles (Jackson Laboratories, #013093) were used in this study. *Sox2-CreER* knock in mice contain the *CreER* fusion gene (causes recombination-estrogen receptor) in place of the *Sox2* coding exon in one allele (Arnold et al., 2011). CAG-tdTomato (Pattabiraman et al., 2014) mice contain a loxP-flanked a STOP cassette in front of a red fluorescent protein variant (tdTomato; Jackson Laboratories, #007914). *Gfi1* (growth factor independent 1 transcriptional repressor)-*Cre* mice, in which one allele of exons 2–5 of *Gfi1* are replaced by the *Cre* gene, were a generous gift from Lin Gan (University of Rochester, Rochester, New York). The *Cre* lines were maintained as heterozygotes and the floxed lines were kept as homozygotes.

All animal experiments were approved by the Institutional Animal Care and Use Committee of Shanghai Jiaotong University School of Medicine. The experiments were carried out in accordance with the National Institute of Health Guide for the Care and Use of Laboratory Animals (NIH Publications No. 80–23). All efforts were made to minimize the number of animals used and their suffering.

Knockout of *Sox2* in HCs *in vivo*

Sox2$^{flox/flox}$ mice were mated with *Gfi-1-Cre* mice to generate *Sox2*$^{+/flox}$; *Gfi-1-Cre* mice with one null allele of *Sox2*. Then, the resultant *Sox2*$^{+/-}$; *Gfi1-Cre* mice were mated to female Sox2$^{flox/flox}$ mice to generate *Sox2*$^{-/flox}$; *Gfi-1-Cre* mutants (*Gfi1-Cre*, *Sox2*^{flox}, or *Sox2* knockout). The homozygous mutants were defined as *Sox2* knockout. Littermates without Cre were used as controls. The effect of *Sox2* knockout was examined at E18, P5, and P60. *Gfi-1-Cre* only mutants were also examined at P5 as controls.

In vivo lineage tracing

CAG-tdTomato reporter mice were crossed with either *Gfi-1-Cre* or *Sox2-CreER* mice. *Gfi1-Cre; tdTomato* mice were examined at P1. To induce gene deletion, *Sox2-Cre-ER: tdTomato* mice received subcutaneous injections of tamoxifen into their dorsal skin (Sigma; 10 μL dissolved at 50 mg/mL in corn oil) at P1 and P2. The utricle was isolated and analyzed at P5.

Histology and immunostaining

Utricles were dissected and immediately fixed for 30 min with 4% paraformaldehyde. Before incubation with antibodies, the utricles were permeabilized with 4% Triton-X-100 for 1 h at room temperature. The primary antibodies used in our experiments were anti-myosinVIIa (1:300; Proteus Biosciences), anti-SOX2 (1:200; Santa Cruz Biotechnology, sc-17320), anti-oncomodulin (1:200; Santa Cruz Biotechnology, sc-7446), β-III-tubulin (1:500, Covance), and anti-calretinin (1:200; Swant Biotech, 7697). The antibodies were diluted in 0.1% Triton-X-100, 0.1% bovine serum albumin (BSA), 5% horse serum in phosphate-buffered saline (PBS). Species-specific Alexa Fluor-conjugated secondary antibodies diluted in PBS were used for detection (1:500; Invitrogen). Images were acquired using a Leica TCSSP5 confocal microscope. The utricles were scanned in the *Z* plane, or in the *Y* plane at the indicated *x–z* line.

Cell counting

Oncomodulin+ HCs, myosin VIIa (MYO7A)+ HCs; Calretin+ calyces; and β-III-tubulin+ calyces were manually counted using Image J software from the z-stack images of the entire utricle. Myosin VIIa appears in utricle HCs at E13.5 and is used an HC marker (Hasson et al., 1997). The striolar and extrastriolar regions were determined using oncomodulin staining. The number of HCs (MYO7A+) or supporting cells (MYO7A−) in three regions (striolar, extrastriolar, and adjacent area of both) in a 0.01-mm^2 area were counted. Type I HCs were counted as MYO7A+ and β-III-tubulin+ calyces. High-magnification images (150×) were used to visualize and count SOX2+ cells. The cell counts were compared

between the *Sox2* knockout mice and littermate control mice without *Cre* expression (wild-type).

Statistical analysis

Data are shown as the mean ± standard deviation (SD) and analyzed using SPSS software (version 19.0 for Windows, IBM Corp., Armonk, NY, USA). We calculated and analyzed the levels of various markers in positive HCs at each age of the utricle in both the control and experimental groups.

We counted the number of MYO7A and SOX2 positive cells in nine visual fields of the experimental group and the control group. The Shapiro-Wilk test was performed to analyze the normality of the data in each group for MYO7A and SOX2 expression in HC at E18, P5, and P60 (Fig. 4). The data of SOX2 expression in E18 and P60 were not normally distributed, a non-parametric test (Mann-Whitney) was performed to analyze the difference in expression of SOX2 between the experimental group and the control group in E18 and P60. The other data were normally distributed, subsequently, Student's *t* test was performed for the statistical analyses of the differences in MYO7A and SOX2 levels between the two groups at different time points.

Myosin VIIa and OCM were calculated at E18 of *Sox2* knockout mice, and the Shapiro-Wilke test was conducted to analyze the normality of the data in each group (Fig. 5). Data were normally distributed, and Student's *t* test was used to statistical analyze the differences in expression of Myosin VIIa and OCM in E18 mice after *Sox2* knockout.

To illustrate the increased number of Type I HCs in the striola at P5. We counted the number of MYO7A and OCM positive cells in eight visual fields of the wild-type (WT), Gfi1-Cre+ , and Gfi1-Cre+ Sox2 flx/flx mice. The Shapiro-Wilke test and Levene's test was performed to analyze the normality and homogeneity of data for MYO7A and OCM for each group in Fig. 6. The data showed a normal distribution; therefore, the differences in the MYO7A and OCM positive HC counts for each group were determined using one-way ANOVA test followed by Dunnett post-hoc test.

We estimated the number of Type I HCs by counting their characteristic calyces visualized by β-tubulin III staining. We counted the number of calyces in OCM+ cells in the striola in the experimental group and the control group at P5 (Fig. 7C left). The number of Type I HCs was calculated as the β-tubulin III+ calyces per total MYO7A+ HCs (Fig. 7C mid). The percentage of calyces in the whole utricle was compared (Fig. 7C right). The Shapiro-Wilk test was performed to analyze the normality of the data. Data were normally distributed, and Student's *t* test was performed for the statistical analyses of the differences of the percent of calyces in the striola, the number of calyces in the utricle, and the percent of calyces in the utricle between the experimental group and the control group.

To illustrate the increased number of Type I HCs in the striola that were maintained in the adult utricle, we counted the number of MYO7A positive cells of *Sox2* knockout and WT mice at P60 (Fig. 8C left). The number of OCM and Calretinin positive cells were counted in the striola in the adult utricle (Fig. 8C mid and right). The Shapiro-Wilk test

was performed to analyze the normality of the data in each group for MYO7A, OCM, and Calretinin. The number of OCM positive cells were not normally distributed, a non-parametric test (Mann-Whitney) was performed to analyze the difference in expression of OCM. The other data were normally distributed, and Student's *t* test was used for the statistical analyses of the difference in expression of Myosin VIIa and Calretinin in P60 mice.

We used characteristic calyces to estimate the number of Type I HCs at P60. The percent of calyces in OCM+ in striola was calculated for each group (Fig. 9C left). The percentage of Type I HCs was calculated as the β-tubulin III+ calyces per total MYO7A+ HCs in the utricle (Fig. 9C mid). The percentage of calyces in the whole utricle was compared (Fig. 9C right). The Shapiro-Wilk test was also performed to analyze the normality of the data in each group. Data were normally distributed, subsequently, Student's t test was used to perform the statistical analyses of the differences in the percent of calyces in the striola, the number of calyces in the utricle, and the percent of calyces in the utricle. A P value < 0.05 was considered statistically significant.

RESULTS

Type I HCs developed from *Sox2* expressing cells.

Sox2 is expressed throughout life in utricular Type II HCs and utricular supporting cells, but not in Type I HCs (Oesterle et al., 2008). Examination of the neonatal utricle (P1) showed SOX2+ and MYO7A+ Type II HCs, and SOX2− but MYO7A+ Type I HCs (Fig. 2A). The striolar Type I HCs express oncomodulin, a calcium-binding protein (Fig. 2B). To determine the origin of Type I HCs in neonates, we traced the lineage of the SOX2-expressing cells at P1 (administration of tamoxifen at P1 and P2). At P5, Type I HCs were labeled by the *Tomato* reporter in *Sox2-CreER*; *tdTomato* mice (Fig. 2C). This result showed that Type I HCs had developed from SOX2-expressing supporting cells or Type II HCs. In the following experiments, we specifically knocked out the expression of *Sox2* in HCs to investigate the role of SOX2 in HC fate in the vestibular system.

Knockout of *Sox2* in HCs

Gfi1 is essential for the differentiation and survival of inner ear HCs (Wallis et al., 2003; Hertzano et al., 2004). *Gfi1* is expressed in both Type I and Type II HCs, but not in supporting cells, with expression onset at E14.5 coinciding with the appearance of vestibular HCs. *Gfi1-Cre* mice have *Cre* in one allele of the *Gfi1* locus, which drives *Cre* expression in HCs, but not in supporting cells (Yang et al., 2010). Examination of a P1 utricle from *Gfi1-Cre*; *CAG-tdTomato* mice showed reporter expression in most HCs, but not in supporting cells (Fig. 3A). *Sox2* is expressed in Type II HCs. Deletion of *Sox2* in Type II HCs was achieved in the $Sox2^{flox}$; *Gfi1-Cre* mutants. Cre-induced recombination at the *loxP* sites flanking the single exon of *Sox2* resulted in a Sox2-null allele (Shaham et al., 2009). The expression of SOX2 decreased in HCs in the *Gfi1-Cre*; $Sox2^{flox}$ mutants as compared to the wild-type utricles (Fig. 3B and C), whereas SOX2 expression in supporting cells remained the same as that in wild-type utricles (Fig. 3D and E).

We further quantified the SOX2 using immunohistochemistry in *Sox2* knockout mutants at three different ages. Type I HCs can be first identified at E18 by immunostaining of oncomodulin. At E18, the number of SOX2+ HCs was 40% of that of the wild-type control (Fig. 4A). The total number of HCs did not increase by the first postnatal week. At P5, SOX2+ HCs constituted 25% of the HCs in the wild-type utricle (Fig. 4B). The degree of *Sox2* deletion in HCs remained the same in adult mice at P60 as P5 (Fig. 4C). The number of HCs in utricle was 118.4 ± 12.0 and 124 ± 17.0 at E18, 111.9 ± 17.3 and 128.6 ± 21.5 at P5, 142.8 ± 23.2 and 141.7 ± 24.0 at P60, in *Gfi1-Cre + Sox2flx/flx* mutants and wild-type respectively, in the three age groups. Knockout of *Sox2* expression in HCs did not change the number of total HCs (Fig. 4, left panel). At all three ages examined (Fig. 4), there was no statistical difference in total HCs between wild-type and *Gfi1-Cre+ Sox2 flx/flx* mutants (E18: $t(16) = 0.803$, $P = 0.434$; P5: $t(16) = 1.811$, $P = 0.089$; P60: $t(16) = 0.100$, $P = 0.922$). The number of SOX2+ HCs in the utricle was 42 ± 12.4 and 74.8 ± 14.2 at E18, 17.4 ± 5.7 and 68.3 ± 12.7 at P5, and 24.4 ± 9.7 and 77.9 ± 15.8 at P60 in *Gfi1-Cre+ Sox2 flx/flx* mutants and wild-type, respectively, in the three age groups. A decrease in the number of SOX2+ HCs was apparent in Gfi1-Cre+ Sox2 flx/flx mice at E18 ($U(9,9) = 3$, $P < 0.001$), P5 ($t(16) = 10.946$, $P < 0.001$), and P60 ($U(9,9) = 0$, $P < 0.001$) (Fig. 4, right panel).

More Type I HCs were generated by *Sox2* knockout during development

To investigate the dynamics of Type I HC generation, we examined the effect of *Sox2* knockout during embryonic development. The onset of HC development could be observed in vestibular organs at E13.5 by sequential expression of *Atoh1*, *Gfi1*, and *Myo7a* (MYO7A) (Wallis et al., 2003). At E18, oncomodulin was detected in Type I utricular HCs in the striolar region (Fig. 5A). *Sox2* knockout in HCs resulted in an expanded striolar region and stronger expression of oncomodulin in the *Sox2* knockout mutants (Fig. 5B). The total number of HCs in the E18 utricle was 1957.0 ± 203.1 and 1932.2 ± 148.1 in *Gfi1-Cre+ Sox2flx/flx* mutants and wild-type, respectively (Fig. 5C left). There was no significant difference in the number of total HCs ($t(8) = 0.221$, $P = 0.831$) (Fig. 5C left). The number of Type I HCs (OCM+ and MYO7A+) in the E18 utricle was 299.4 ± 57.3 and 127.4 ± 21.1 in *Gfi1-Cre+ Sox2flx/flx* mutants and wild-type, respectively (Fig. 5C right). The number of Type I HCs (OCM+ and MYO7A+) in *Gfi-1-Cre+ Sox2 flx/flx* mutants was 235% of that in the wild-type mice ($t(8) = 6.295$, $P = 0.001$) (Fig. 5C right).

Sox2 knockout increased the number of Type I HCs in neonates.

HCs continue to be added after birth, mostly during the first postnatal week (Burns et al., 2012). By P5, loss of *Sox2* expanded the striolar region, as defined by oncomodulin+ cells, and the number of Type I HCs (Fig. 6A and C). *Gfi-1 – Cre* mice without the *Sox2* mutation had similar number of oncomodulin+ cells and MYO7A+ HCs as the wild-type (Fig. 6B). The total number of HCs in the P5 utricle was 2196.5 ± 176.7, 2120.8 ± 200.7, and 2087.1+ 161.7 in wild-type, Gfi1-Cre+ , and Gfi1-Cre+ Sox2flx/flx mutants, respectively (Fig. 6D left). There was no significant differences in the total number of HCs (MYO7A+) among the three groups ($F(2,21) = 0.792$, $P = 0.468$) (Fig. 6D left). The number of Type I HCs in the P5 utricle was 202.9 ± 65.1, 210.4 ± 45.9, and 494.1 + 97.7 in wild-type, *Gfi1-Cre+*, and *Gfi1-Cre+ Sox2flx/flx* mutants, respectively (Fig. 6D right). The total number of Type I HCs (OCM) increased in *Sox2* knockout mice (Fig. 6D right). Striolar Type I HCs

(oncomodulin+) had increased to 244% of that in the wild-type. There were significant differences between *Sox2* knockout mice and the other two groups ($F(2,21) = 35.357$, $P < 0.001$) (Fig. 6D right).

Type I HCs have calyces at their lateral and basal surfaces. Oncomodulin is a marker for the Type I HCs in the striola region. In the wild-type, 92 ± 3.14% of oncomodulin+ HCs formed calyces with afferent endings that were stained with β-III-tubulin (Fig. 7A and C). Even though the number of oncomodulin+ HCs increased following *Sox2* knockout, the percentage of calyces in the oncomodulin+ cells remained similar to that of the wild-type (89.9 ± 1.2%, Fig. 7B and C). In the wild-type and mutant utricles, 92% and 89.9% of the OCM cells had calyces, respectively ($t(8) = 1.398$, $P = 0.219$) (Fig. 7C left). This confirmed that more stiolar Type I HCs were generated after *Sox2* knockout. β-III-tubulin could label calyces in both the striolar and extrastriolar regions. We found that *Sox2* knockout efficiency was similar at the striolar *vs.* extrastriolar regions (Fig. 4); therefore, the number of Type I HCs was also quantified in the extrastriolar region. We found more Type I HCs in the extrastriola region compared with that in the wild-type mice. The total number of Type I HCs with β-III-tubulin+ calyces in the *Sox2* knockout mice was 157% of that in the wild-type (1337.6 ± 94.9 *vs.* 849.8 ± 50.4, Fig. 7C mid). The number of Type I HCs was calculated as the β-tubulin III+ calyces per total MYO7A+ HCs ($t(8) = 10.153$, $P < 0.001$) (Fig. 7C mid). The percentage of Type I HCs increased significantly in the whole utricle from 47.3 ± 2.4% in the wild-type to 59.1 ± 1.6% after *Sox2* knockout (Fig. 7C right). The percentage of Type I HCs increased from 47.3% in the wild-type to 59.1% in the Sox2 mutants ($t(8) = 9.057$, $P < 0.001$) (Fig. 7C right).

Increased Type I HCs persist into adulthood

HCs continue to mature as functional Type I and Type IIs after birth. To examine whether the effect of *Sox2* knockout can persist into adulthood, we examined Type I HCs in utricles at P60. In adults, calyces show strong expression of calretinin, a calcium-binding protein. At P60, oncomodulin+ cells and calretinin+ calyces were detected in Type I utricular HCs in the striolar region (Fig. 8A). *Sox2* knockout in HCs resulted in an expanded striolar region and stronger expression of oncomodulin+ cells and calretinin+ calyces in the *Sox2* knockout mutants (Fig. 8B). The total number of HCs in the P60 utricle was 1972.6 ± 140.1 and 2106.3 ± 152.1, respectively, in Gfi1-Cre+ Sox2flx/flx mutants and wild-type (Fig. 8C left). The total number of HCs (MyoVIIa+) was unchanged ($t(8) = 1.500$, $P = 0.168$) (Fig. 8C left). The number of OCM+ cells in the P60 utricle was 247.4 ± 38.0 and 154.3 ± 20.8 in *Gfi1-Cre+ Sox2flx/flx* mutants and wild-type, respectively (Fig. 8C mid). The number of OCM + and Calretinin+ cells in the P60 utricle was 193.8 ± 41.5 and 120.2 ± 20.0 in Gfi1-Cre+ Sox2flx/flx mutants and wild-type, respectively (Fig. 8C right). Quantification revealed that the utricles of *Sox2* knockout mice had 160.3% OCM+ Type I HCs ($U(5,5) = 0$, $P = 0.004$) (Fig. 8C mid) and 161.2 % calyces ($t(8) = 3.57$, $P = 0.007$) (Fig. 8C right) as compared with wild-type mice. From P5 to P60, we observed a decrease in the number of oncomodulin+ HCs both in the wild-type (75% of P5) and *Sox2* knockout mice, with more pronounced changes in the *Sox2* knockout mice (50% of P5) (Figs. 6C *vs.* 8C). This suggested that not all Type I HCs generated in the striolar region during normal maturation or in *Sox2* mutant maintained their fate into adulthood.

Type I HCs were further characterized by another calyx marker, β-III-tubulin. Consistent with calretinin-labeled calyces, the number of oncomodulin+/β-III-tubulin+ Type I HCs in the striolar region increased in the *Sox2* knockout mutants (Fig. 9A *vs.* B). The percentage of β-III-tubulin+ calyces among oncomodulin+ HCs was similar in the wild-type utricles and the *Sox2* knockout mutants (89.3 ± 1.3% in the *Sox2* knockout *vs.* 91.5 ± 2.1% in the wild-type) ($t(8) = 2.041$, $P = 0.076$) (Fig. 9C left). β-III-tubulin labels calyces in both striolar and extrastriolar regions, which allows assessment of Type I HCs in the entire utricle. Quantification of Type I HCs in *Sox2* knockout mutant and wild-type utricles revealed that the total number of calyx+ cells in the P60 utricle was 1252.6 ± 142.0 and 1051.2 ± 63.9 in Gfi1-Cre+ Sox2flx/flx mutants and wild-type, respectively (Fig. 9C mid). The total number of cells with a calyx in the *Sox2* mutant was 119% of that in the wild-type utricle ($t(8) = 2.893$, $P = 0.02$) (Fig. 9C mid). For the entire utricle, Type I HCs with calyces increased from 53.6 ± 2.3% in the wild-type to 64.3 ± 1.7% in the *Sox2* knockout mutants. ($t(8) = 8.451$, $P < 0.001$) (Fig. 9C right). In the cross-section view, oncomodulin+ Type I HCs was enveloped by calyces, which expressed calretinin or β-III-tubulin+ (Fig. 9D and E). In the *Sox2* knockout mutants, the anatomical features of oncomodulin+ Type I HCs were similar to those of the wild type Type I HCs, showing calretinin and β-III-tubulin+ calyces (Fig. 9D′ and E′).

DISCUSSION

The molecular pathways and originating cells for the development of the highly specialized Type I HCs of the amniote vestibular systems remain unknown. Candidates include progenitor cells, supporting cells, and even Type II HCs (Eatock and Rusch, 1997; Rusch et al., 1998; Eatock and Hurley, 2003). Type II HCs, similar to progenitor and support cells, continue to express SOX2 postnatally; however, Type I cells, like mammalian cochlear HCs, experience a reduction in SOX2 expression subsequent to the initiation of HC transcription factor ATOH1 expression. Zebrafish express Sox2 in sensory progenitors and supporting cells, but not in HCs (Hernandez et al., 2007). Knockdown of *sox2* in zebrafish did not prevent HC production during development, but led to sporadic death of differentiated HCs. Furthermore, Sox2 depletion inhibits transdifferentiation of supporting cells into HCs during regeneration (Millimaki et al., 2010). We found that hair-cell-specific knockout of Sox2 changed Type II HCs into Type I HCs, demonstrating that SOX2 controls cell fate decisions in vestibular HCs. Using a knockout strategy that suppresses *Sox2* only in HCs after *Gfi1* expression (early in the development of HCs, at E14.5), the expansion of striolar Type I HCs was evident as early as E18 and persisted into adulthood.

SOX2 in sequential differentiation of inner ear cells

SOX2 plays dynamic roles during inner ear development. Animals lacking *Sox2* expression failed to establish a prosensory domain without HCs and supporting cells, whereas the animals with reduced *Sox2* expression showed abnormal development with disorganized and fewer HCs (Kiernan et al., 2005). Upon specification of the otic placode, SOX2 maintains the prosensory progenitor fate.

However, recent studies have shown that SOX2 acts upstream of ATOH1 and is important for the differentiation of HCs (Ahmed et al., 2012; Neves et al., 2012; Kempfle et al., 2016). *Sox2* knockout prevented the differentiation of HCs, even after progenitor cells had been established (Kempfle et al., 2016). In the cochlea, SOX2 antagonizes *Atoh1* expression and prevents the differentiation of progenitor cells into HCs (Dabdoub et al., 2008). After birth, knockout of *Sox2* promoted the proliferation of supporting cells via down regulation of *P27kip* (encoding cyclin dependent kinase inhibitor 1B) (Liu et al., 2012) without an effect on cochlear HC differentiation. *Sox4* and *Sox11* expression are also necessary for HC development in the inner ear, and their overexpression leads to the proliferation of supporting cells and HC production in adult mouse utricles (Gnedeva and Hudspeth, 2015).

In our study of cell fate determination by SOX2, we confirmed that SOX2 is expressed in supporting cells and Type II HCs. Type I HCs are defined as oncomodulin+ in the striola and are enveloped by calyces. Oncomodulin immunoreactivity could be detected Type I HCs in the striolar region starting at E18 but was reduced in the older adult age (Simmons et al, 2010). Hoffman et al. (2018) showed that oncomodulin also labeled a small percentage of Type II HCs. Our study found that the number of oncomodulin+ cells was reduced in both wild-type and *Sox2* knockout adults. About 10% of oncomodulin+ cells were not enveloped by calyces. We assumed that these were Type II HCs. Matern et al. (2017) showed that *Gfi1-Cre* haploinsufficienciency animals presented progressive hearing loss, but had no decline in vestibular function up to 10 months. The present study also showed that at P5, *Gfi1-Cre* animals had a similar number of HCs and oncomodulin+ cells as the wild-type animals, which is consistent with Matern's finding on normal vestibular HC development and function in *Gfi1-Cre* animals. We deleted Sox2 in Type II HCs in a *Gfi1-Cre* background, which is specific for HCs. This revealed a role for SOX2 in the formation of new type I HCs at the expense of type II HCs. The phenotypic shift of Type II HCs toward Type I HCs was observed at E18, P5, and P60. The total number of HCs per utricle did not change, confirming that the additional cells had arisen through a phenotypic change of Type II HCs into Type I HCs. These data suggested that SOX2 expression determines Type I *vs*. Type II HC fate in the mouse utricle. The increased number of Type I HCs after *Sox2* knockdown in HCs might result from a change in cell fate, loss of Type II identity, premature differentiation of Type I HCs, or a mixed phenotype, with both Type I and Type II properties. The precise mechanism for the preservation of Type II HC fate and the changes in cell fate resulting from genetic deletion of *Sox2* require further study.

SOX1, SOX2, and SOX3 (members of the SoxB1 family) are markers of neural progenitors throughout the vertebrate CNS. SOX2 becomes largely restricted to the neuroectoderm, sensory placodes, and gut endoderm during development (Avilion et al., 2003). SOX2 directs bipotential axial stem cells toward a neural plate fate. Constitutive expression of Sox2 maintains progenitor fate and results in inhibition of neuronal differentiation (Graham et al., 2003). Conversely, inhibition of Sox2 expression leads to cell cycle exit, delamination of progenitors from the ventricular zone, and expression of neuronal differentiation markers (Graham et al., 2003). Furthermore, SOX2 might be important for the differentiation of neuronal subtypes. In addition, direct reprogramming of fibroblasts to neural stem cells acts via ectopic *Sox2* expression. For example, temporal overexpression of octamer-binding protein 4 (*Oct4*) , Kruppel like factor 4 (*Klf4*), *Sox2*, and MYC proto-oncogene, BHLH

transcription factor (*c-Myc*) in mouse embryonic fibroblasts induced neural stem cells to express paired box 6 (*Pax6*), and a PLZF (promyelocytic leukemia zinc finger) gene, without involving a transient pluripotent intermediate stage (Kim et al., 2011; Thier et al., 2012).

The effects of SOX2 depend on its level

The effector activity of SOX2 is exerted through DNA binding and is dependent on its abundance (Ambrosetti et al., 1997; Boer et al., 2007). SOX2 is expressed widely in the embryos and in the progenitor cells of various organs, as well as in the developing and mature nervous system. This could be caused by competing factors that fine tune *Sox2* expression. However, unlike excess *Notch*, excess *Sox2* did not inhibit maturation of HCs once they were formed (Savoy-Burke et al., 2014). *Sox2* haploinsufficiency delayed terminal mitosis in the cochlea and was a permissive signal for Wnt-mediated cell proliferation and new hair cell generation (Atkinson et al., 2018). In the experiments described here, Type I HCs were produced after deletion of both alleles of *Sox2*.

SOX2 maintains Type II HC identity

SOX2 counteracts HC specification in the organ of Corti; however, it is crucial to maintain the fate of Type II HCs in the vestibular system. The results showed that although SOX2 immunoreactivity became undetectable in 80% of HCs, not all Type II HCs changed into Type I HCs. It is surprising that the change from one cell type to another is controlled by a single transcription factor. *Sox2*, *Sox9*, and *Sox10* have been reported to be co-expressed in the oticplacode, cochlear duct, and later in cochlear supporting cells in mice and humans (Barrionuevo et al., 2008; Breuskin et al., 2009; Mak et al., 2009; Locher et al., 2013). It would be interesting to determine the expression patterns of other *Sox* factors in Type II HCs and the cofactors responsible for maintaining Type II HCs.

Accumulating data suggest the pathways and factors that control cell fate decisions between supporting cells and HCs; however, there is little information on the factors that specify HC subtypes. Our findings demonstrated that SOX2 plays a critical role in the adoption of Type II *vs.* Type I HC fate. During utricular regeneration, new HCs are mainly Type II, not Type I (Golub et al., 2012). Type I HCs respond to rapid signals and underlie fast conduction in the vestibular organ. Although further studies are required to investigate the mechanism of action of SOX2 in HCs, the data reported here suggest that downregulation of *Sox2* expression is a potential strategy to regenerate Type I HCs from Type II HCs, which might accumulate after stimulating regeneration.

ACKNOWLEDGEMENTS

We thank Dr. Ruth Anne Eatock for critical reading and thorough editing, and Dr. Joseph C Burns and Dr. Jennifer Stone for helpful comments.

FUNDING

This work was supported by grants from the National Natural Science Foundation of China [grant numbers 81570906, 81330023, 81271088, 81200742]; the Natural Science Foundation of Shanghai [grant numbers 17ZR1418100, 14DJ1400200, 11ZR1423600]; Shanghai Shen Kang Hospital Development Center [grant number SHDC12013109]; and Shanghai Key Laboratory of Translational Medicine on Ear and Nose Diseases Foundation [grant number 14DZ2260300].

Abbreviations:

HCs	hair cells
BSA	bovine serum albumin
PBS	phosphate-buffered saline
SOX2	SRY-box 2
GFI1	growth factor independent 1 transcriptional repressor
Cre	causes recombination
ATOH1	atonal BHLH transcription factor 1
POU4F3	POU class 4 homeobox 3
loxP	locus of X-over P1
ER	estrogen receptor
MYO7A	myosin VIIa
OCT4	octamer-binding protein 4
KLF4	Kruppel like factor 4
c-MYC	MYC proto-oncogene, BHLH transcription factor
PAX6	paired box 6

REFERENCES

Ahmed M, Wong EY, Sun J, Xu J, Wang F, Xu PX (2012) Eya1-Six1 interaction is sufficient to induce hair cell fate in the cochlea by activating Atoh1 expression in cooperation with Sox2. Dev Cell 22:377–390. [PubMed: 22340499]

Ambrosetti D-C, Basilico C, Dailey L (1997) Synergistic activation of the fibroblast growth factor 4 enhancer by Sox2 and Oct-3 depends on protein-protein interactions facilitated by a specific spatial arrangement of factor binding sites. Mol Cell Biol 17:6321–6329. [PubMed: 9343393]

Arnold K, Sarkar A, Yram MA, Polo JM, Bronson R, Sengupta S, Seandel M, Geijsen N, et al. (2011) Sox2(+) adult stem and progenitor cells are important for tissue regeneration and survival of mice. Cell Stem Cell 9:317–329. [PubMed: 21982232]

Atkinson PJ, Dong Y, Gu S, Liu W, Najarro EH, Udagawa T, Cheng AG (2018) Sox2 haploinsufficiency primes regeneration and Wnt responsiveness in the mouse cochlea. J Clin Invest 128.

Avilion AA, Nicolis SK, Pevny LH, Lidia P, Nigel V, Robin LB (2003) Multipotent cell lineages in early mouse development depend on SOX2 function. Genes Dev 17:126–140. [PubMed: 12514105]

Barrionuevo F, Naumann A, Bagheri-Fam S, Speth V, Taketo MM, Scherer G, Neubuser A (2008) Sox9 is required for invagination of the otic placode in mice. Dev Biol 317:213–224. [PubMed: 18377888]

Boer B, Kopp J, Mallanna S, Desler M, Chakravarthy H, Wilder PJ, Bernadt C, Rizzino A (2007) Elevating the levels of Sox2 in embryonal carcinoma cells and embryonic stem cells inhibits the expression of Sox2:Oct-3/4 target genes. Nucleic Acids Res 35:1773–1786. [PubMed: 17324942]

Boyer LA, Lee TI, Cole MF, Johnstone SE, Levine SS, Zucker JP, Guenther MG, Kumar RM, et al. (2005) Core transcriptional regulatory circuitry in human embryonic stem cells. Cell 122:947–956. [PubMed: 16153702]

Breuskin I, Bodson M, Thelen N, Thiry M, Borgs L, Nguyen L, Lefebvre PP, Malgrange B (2009) Sox10 promotes the survival of cochlear progenitors during the establishment of the organ of Corti. Dev Biol 335:327–339. [PubMed: 19748502]

Burns JC, On D, Baker W, Collado MS, Corwin JT (2012) Over half the hair cells in the mouse utricle first appear after birth, with significant numbers originating from early postnatal mitotic production in peripheral and striolar growth zones. J Assoc Res Otolaryngol 13:609–627. [PubMed: 22752453]

Burns JC, Stone JS (2017) Development and regeneration of vestibular hair cells in mammals. Semin Cell Dev Biol 65:96–105. [PubMed: 27864084]

Contini D, Zampini V, Tavazzani E, Magistretti J, Russo G, Prigioni I, Masetto S (2012) Intercellular K(+) accumulation depolarizes Type I vestibular hair cells and their associated afferent nerve calyx. Neuroscience 227:232–246. [PubMed: 23032932]

Dabdoub A, Puligilla C, Jones JM, Fritzsch B, Cheah KS, Pevny LH, Kelley MW (2008) Sox2 signaling in prosensory domain specification and subsequent hair cell differentiation in the developing cochlea. Proc Natl Acad Sci USA 105:18396–18401. [PubMed: 19011097]

Denman-Johnson K, Forge A (1999) Establishment of hair bundle polarity and orientation in the developing vestibular system of the mouse. J Neurocytol 28:821–835. [PubMed: 10900087]

Desai SS, Zeh C, Lysakowski A (2005) Comparative morphology of rodent vestibular periphery. I. Saccular and utricular maculae. J Neurophysiol 93:251–266. [PubMed: 15240767]

Eatock RA, Hurley KM (2003) Functional development of hair cells. Curr Top Dev Biol 57:389–448. [PubMed: 14674488]

Eatock RA, Rusch A (1997) Developmental changes in the physiology of hair cells. Semin Cell Dev Biol 8:265–275. [PubMed: 10024489]

Eatock RA, Songer JE (2011) Vestibular hair cells and afferents: two channels for head motion signals. Annu Rev Neurosci 34:501–534. [PubMed: 21469959]

Gnedeva K, Hudspeth A (2015) SoxC transcription factors are essential for the development of the inner ear. Proc Natl Acad Sci USA 112:14066–14071. [PubMed: 26504244]

Golub JS, Tong L, Ngyuen TB, Hume CR, Palmiter RD, Rubel EW, Stone JS (2012) Hair cell replacement in adult mouse utricles after targeted ablation of hair cells with diphtheria toxin. J Neurosci 32:15093–15105. [PubMed: 23100430]

Graham V, Khudyakov J, Ellis P, Pevny L (2003) SOX2 functions to maintain neural progenitor identity. Neuron 39:749–765. [PubMed: 12948443]

Hasson T, Gillespie PG, Garcia JA, MacDonald RB, Zhao Y-d, Yee AG, Mooseker MS, Corey DP (1997) Unconventional myosins in inner-ear sensory epithelia. J Cell Biol 137:1287–1307. [PubMed: 9182663]

Hernandez PP, Olivari FA, Sarrazin AF, Sandoval PC, Allende ML (2007) Regeneration in zebrafish lateral line neuromasts: expression of the neural progenitor cell marker sox2 and proliferation-dependent and-independent mechanisms of hair cell renewal. Dev Neurobiol 67:637–654. [PubMed: 17443814]

Hertzano R, Montcouquiol M, Rashi-Elkeles S, Elkon R, Yucel R, Frankel WN, Rechavi G, Moroy T, et al. (2004) Transcription profiling of inner ears from Pou4f3(ddl/ddl) identifies Gfi1 as a target of the Pou4f3 deafness gene. Hum Mol Genet 13:2143–2153. [PubMed: 15254021]

Hoffman LF, Choy KR, Sultemeier DR, Simmons DD (2018) Oncomodulin expression reveals new insights into the cellular organization of the murine Utricle Striola. J Assoc Res Otolaryngol 19:33–51. [PubMed: 29318409]

Holt JC, Xue JT, Brichta AM, Goldberg JM (2006) Transmission between type II hair cells and bouton afferents in the turtle posterior crista. J Neurophysiol 95:428–452. [PubMed: 16177177]

Hume CR, Bratt DL, Oesterle EC (2007) Expression of LHX3 and SOX2 during mouse inner ear development. Gene Expr Patterns 7:798–807. [PubMed: 17604700]

Kempfle JS, Turban JL, Edge AS (2016) Sox2 in the differentiation of cochlear progenitor cells. Sci Rep 6:23293. [PubMed: 26988140]

Kevetter GA, Leonard RB (2002) Decreased expression of calretinin and calbindin in the labyrinth of old gerbils. Brain Res 957: 362–365. [PubMed: 12445979]

Kiernan AE, Pelling AL, Leung KK, Tang AS, Bell DM, Tease C, Lovell-Badge R, Steel KP, et al. (2005) Sox2 is required for sensory organ development in the mammalian inner ear. Nature 434:1031. [PubMed: 15846349]

Kim J, Efe JA, Zhu S, Talantova M, Yuan X, Wang S, Lipton SA, Zhang K, et al. (2011) Direct reprogramming of mouse fibroblasts to neural progenitors. Proc Natl Acad Sci USA 108:7838–7843. [PubMed: 21521790]

Kirk ME, Meredith FL, Benke TA, Rennie KJ (2017) AMPA receptor-mediated rapid EPSCs in vestibular calyx afferents. J Neurophysiol 117:2312–2323. [PubMed: 28298303]

Li GQ, Meredith FL, Rennie KJ (2010) Development of K+ and Na+ conductances in rodent postnatal semicircular canal type I hair cells. Am J Physiol Regul Integr Comp Physiol 298:R351–R358. [PubMed: 19939976]

Liu Z, Walters BJ, Owen T, Brimble MA, Steigelman KA, Zhang L, Mellado Lagarde MM, et al. (2012) Regulation of p27Kip1 by Sox2 maintains quiescence of inner pillar cells in the murine auditory sensory epithelium. J Neurosci 32:10530–10540. [PubMed: 22855803]

Locher H, Frijns JH, van Iperen L, de Groot JC, Huisman MA, de Sousa Lopes SMC (2013) Neurosensory development and cell fate determination in the human cochlea. Neural Dev 8:20. [PubMed: 24131517]

Lysakowski A, Goldberg JM (1997) A regional ultrastructural analysis of the cellular and synaptic architecture in the chinchilla cristae ampullares. J Comp Neurol 389:419–443. [PubMed: 9414004]

Mak AC, Szeto IY, Fritzsch B, Cheah KS (2009) Differential and overlapping expression pattern of SOX2 and SOX9 in inner ear development. Gene Expr Patterns 9:444–453. [PubMed: 19427409]

Matern M, Vijayakumar S, Margulies Z, Milon B, Song Y, Elkon R, Zhang X, Jones SM, Hertzano R (2017) Gfi1Cre mice have early onset progressive hearing loss and induce recombination in numerous inner ear non-hair cells. Sci Rep. 7:42079. [PubMed: 28181545]

Mbiene J-P, Favre D, Sans A (1984) The pattern of ciliary development in fetal mouse vestibular receptors. Anat Embryol 170:229–238.

Millimaki BB, Sweet EM, Riley BB (2010) Sox2 is required for maintenance and regeneration, but not initial development, of hair cells in the zebrafish inner ear. Dev Biol 338:262–269. [PubMed: 20025865]

Monzack EL, Cunningham LL (2013) Lead roles for supporting actors: critical functions of inner ear supporting cells. Hear Res 303:20–29. [PubMed: 23347917]

Neves J, Uchikawa M, Bigas A, Giraldez F (2012) The prosensory function of Sox2 in the chicken inner ear relies on the direct regulation of Atoh1. PLoS One 7 e30871. [PubMed: 22292066]

Oesterle EC, Campbell S, Taylor RR, Forge A, Hume CR (2008) Sox2 and JAGGED1 expression in normal and drug-damaged adult mouse inner ear. J Assoc Res Otolaryngol 9:65–89. [PubMed: 18157569]

Pattabiraman K, Golonzhka O, Lindtner S, Nord AS, Taher L, Hoch R, Silberberg SN, Zhang D, et al. (2014) Transcriptional regulation of enhancers active in protodomains of the developing cerebral cortex. Neuron 82:989–1003. [PubMed: 24814534]

Rusch A, Lysakowski A, Eatock RA (1998) Postnatal development of type I and type II hair cells in the mouse utricle: acquisition of voltage-gated conductances and differentiated morphology. J Neurosci 18:7487–7501. [PubMed: 9736667]

Sans A, Chat M (1982) Analysis of temporal and spatial patterns of rat vestibular hair cell differentiation by tritiated thymidine radioautography. J Comp Neurol 206:1–8. [PubMed: 6124561]

Savoy-Burke G, Gilels FA, Pan W, Pratt D, Que J, Gan L, White PM, Kiernan AE (2014) Activated notch causes deafness by promoting a supporting cell phenotype in developing auditory hair cells. PLoS One 9 e108160. [PubMed: 25264928]

Shaham O, Smith AN, Robinson ML, Taketo MM, Lang RA, Ashery-Padan R (2009) Pax6 is essential for lens fiber cell differentiation. Development 136:2567–2578. [PubMed: 19570848]

Simmons DD, Tong B, Schrader AD, Hornak AJ (2010) Oncomodulin identifies different hair cell types in the mammalian inner ear. J Comp Neurol 518:3785–3802. [PubMed: 20653034]

Thier M, Wörsdörfer P, Lakes YB, Gorris R, Herms S, Opitz T, Seiferling D, Quandel T, et al. (2012) Direct conversion of fibroblasts into stably expandable neural stem cells. Cell Stem Cell 10:473–479. [PubMed: 22445518]

Wallis D, Hamblen M, Zhou Y, Venken KJ, Schumacher A, Grimes HL, Zoghbi HY, Orkin SH, et al. (2003) The zinc finger transcription factor Gfi1, implicated in lymphomagenesis, is required for inner ear hair cell differentiation and survival. Development 130:221–232. [PubMed: 12441305]

Wan G, Corfas G, Stone JS (2013) Inner ear supporting cells: rethinking the silent majority. In: Seminars in cell & developmental biology. Elsevier. p. 448–459.

Yamashita M, Ohmori H (1990) Synaptic responses to mechanical stimulation in calyceal and bouton type vestibular afferents studied in an isolated preparation of semicircular canal ampullae of chicken. Exp Brain Res 80:475–488. [PubMed: 2387349]

Yang H, Gan J, Xie X, Deng M, Feng L, Chen X, Gao Z, Gan L (2010) Gfi1-Cre knock-in mouse line: a tool for inner ear hair cell-specific gene deletion. Genesis 48:400–406. [PubMed: 20533399]

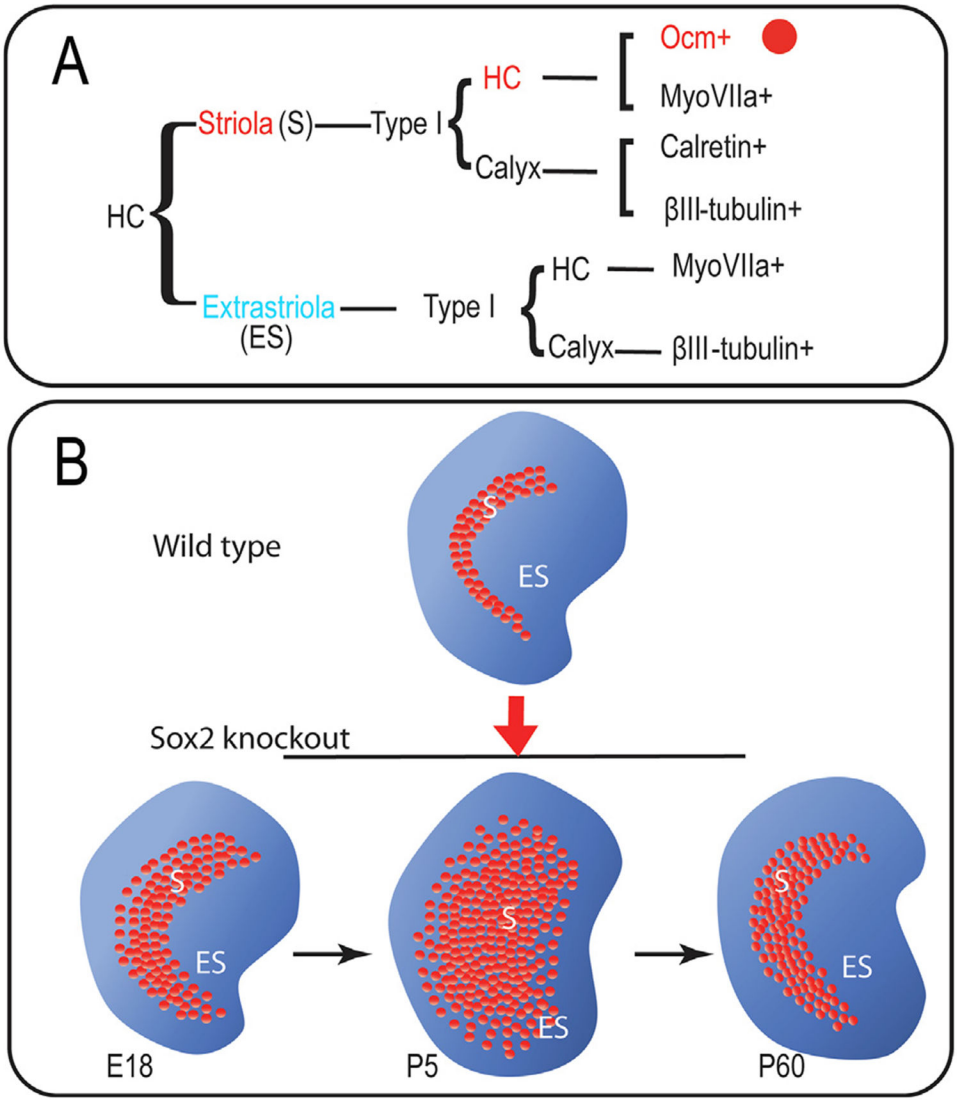

Fig. 1.

Schematic representation of mouse utricular macula following *Sox2* knockout. (A) HCs are distributed in the striola (S) and extrastriola (ES). The afferent nerve ending forms characteristic calyces with Type I HCs. Type I HCs in the striolar region are labeled with oncomodulin (Ocm) and myosin VIIa (Myo VIIa) and calyces are labeled with calretinin and β-tubulin III. In the extrastriolar region, Type I HCs are labeled with myosin VIIa and calyces are labeled with β-tubulin III. (B) Following *Sox2* knockout in Type II HCs, an increase in the number of Type I HCs was observed. Increased numbers of Type I HCs were maintained until adulthood. SOX2, SRY-box 2; HC, hair cell.

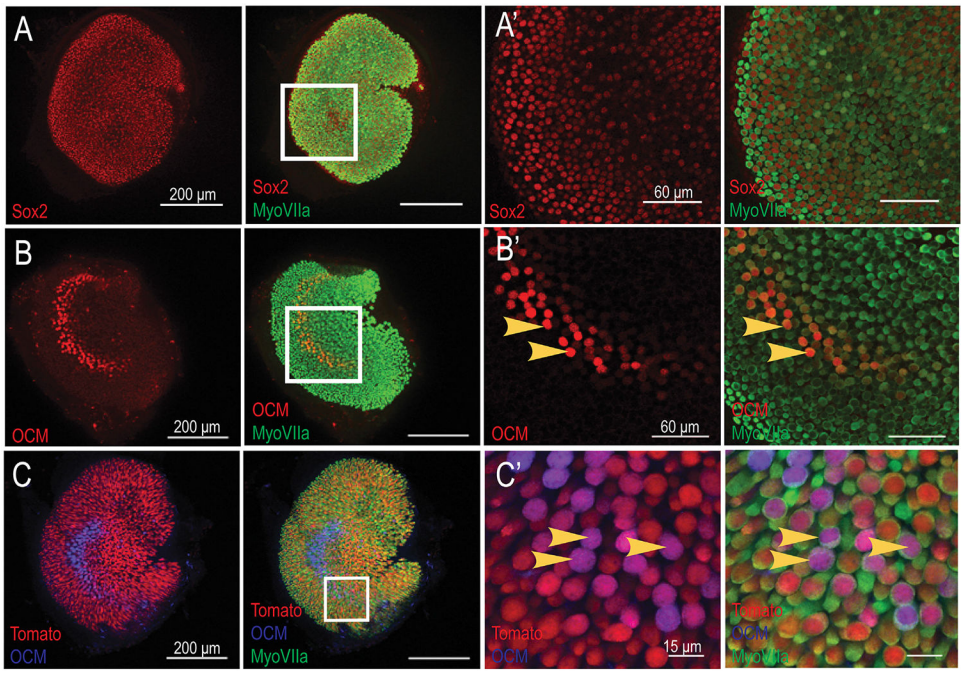

Fig. 2.

Type I HCs developed from *Sox2* expressing cells in the postnatal utricle. (A and A′) SOX2 is expressed in Type II HCs in the striolar and extrastriolar regions in P1 utricles, as assessed at low (A) and high (A′) magnification. B and B′ Type I HCs in the striolar region expressed oncomodulin at low (B) and high (B′) magnification. Arrows point to oncomodulin+ cells. (C and C′). Lineage tracing of SOX2 expressing cells *in Sox2-CreER*; *tdTomato* mice with tamoxifen administration at P1. Oncomodulin+ Type I HCs in the striola were labeled by tdTomato at P5 (arrows), demonstrating that Type I HCs are derived from SOX2-expressing cells. Utricles are shown at low (C) and high (C′) magnification. HCs were stained with anti-myosin VIIa antibodies. SOX2, SRY-box 2; HC, hair cell.

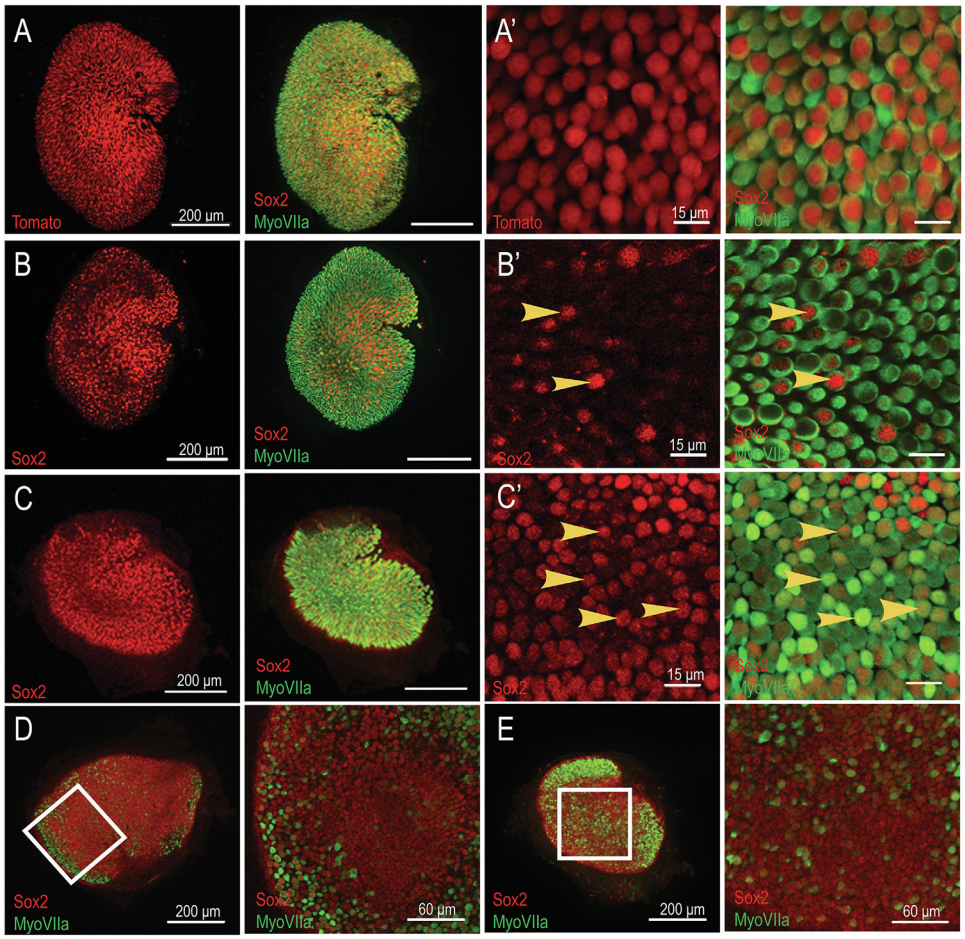

Fig. 3.

Knockout of *Sox2* expression in HCs using *Gfi1-Cre*. (A) Gfi drives Cre expression in HCs. At P1, HCs expressed tdTomato (Tomato) in *GfH-Cre*; tdTomato mice. (A′) High-magnification images. (B) Knockout of Sox2 in HCs. At P5, SOX2 expression in *Gfi1-Cre*; $Sox2^{flox}$ mice was decreased in HCs. (B′) High magnification images. (C) Wild-type $Sox2^{flox}$ littermates showing SOX2 expression in Type II HCs. (C′) High-magnification images. (D) No change in SOX2 expression was observed in supporting cells in the *Gfi1-Cre*; $Sox2^{flox}$ mutants. (E) SOX2 expression in the supporting cells in the wild-type. Images were taken at the supporting cell plane. Hair cells were stained with anti-myosin VIIa antibodies. Arrows point to SOX2+ and myosin VIIa+ HCs. SOX2, SRY-box 2; HC, hair cell; *Gfi1*, growth factor independent 1 transcriptional repressor; *Cre*, causes recombination.

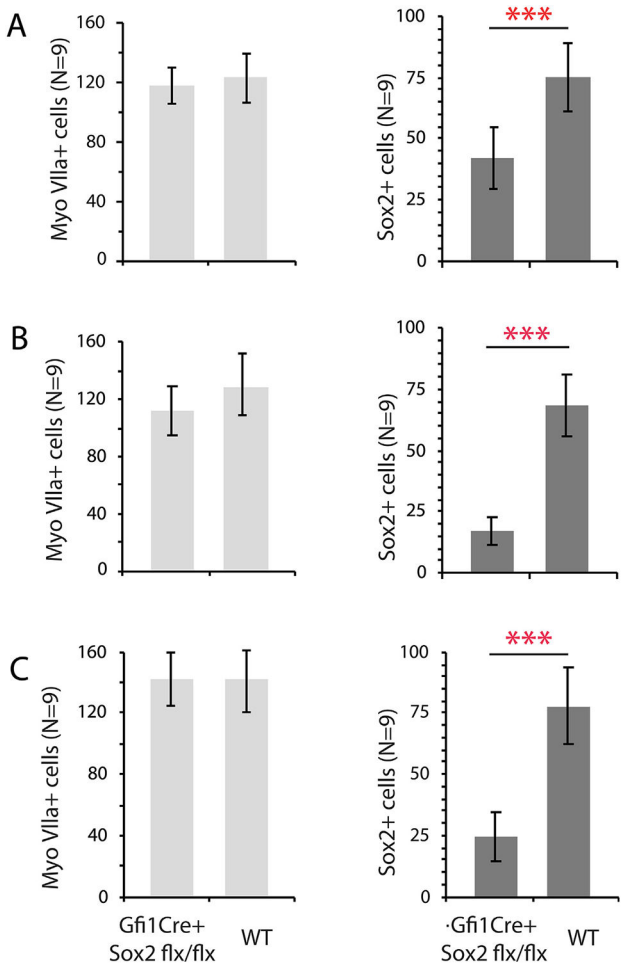

Fig. 4.

Quantification of SOX2 expression in HCs. Gfi1 is expressed in utricular HCs at E14.5, concurrent with the time of HC differentiation. HCs and SOX2+ HCs were counted. (A) Fewer SOX2+ HCs in *Gfi1-Cre*; *Sox2*^{flox} mutants at E18 ($U(9,9) = 3$, $P < 0.001$). (B) A decrease in the number of SOX2+ HCs was apparent in *Gfi1-Cre*; *Sox2*^{flox} mice at P5 ($t(16) = 10.946$, $P < 0.001$). (C) Knockout of SOX2 was maintained to P60 ($U(9,9) = 0$, $P < 0.001$). At all three ages examined, there was no statistical difference in total HCs between wild-type and *Gfi1-Cre*; *Sox2*^{flox} mutants. HCs were stained with MYO7A antibodies. SOX2 expression was detected using antibody staining. Values and error bars represent the means ± SD SOX2, SRY-box 2; HC, hair cell; *Gfi1*, growth factor independent 1 transcriptional repressor; *Cre*, causes recombination. *** marks $P < 0.001$, ** marks $P < 0.01$, * marks $P < 0.05$.

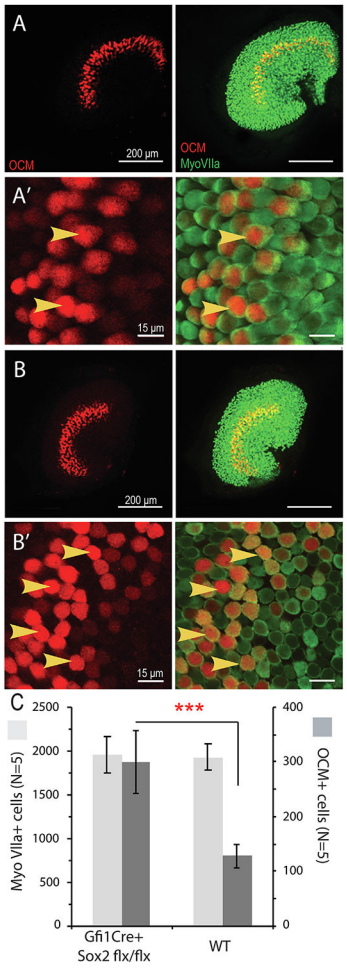

Fig. 5.

Increase in Type I HCs at E18 in *Sox2* knockout mice. HCs express oncomodulin at E18. (A) Oncomodulin+ HCs in the striolar region in the wild-type utricles. (A′) High magnification images of A in the striolar region. (B) More oncomodulin+ HCs were observed in the *Gfi-1-Cre*; $Sox2^{flox}$ mutants. (B′) High magnification images. (C) The number of Type I HCs (oncomodulin+ and myosin VIIa+) in *Gfi-1-Cre;* $Sox2^{flox}$ mutants was 235% of that in the wild-type mice ($t(8) = 6.295$, $P = 0.001$). There was no significant difference in the number of total HCs ($t(8) = 0.221$, $P = 0.831$). Arrows point to oncomodulin+ and myosin VIIa+ cells. Values and error bars represent the means ± SD. SOX2, SRY-box 2; HC, hair cell; *Gfi1*, growth factor independent 1 transcriptional repressor; *Cre*, causes recombination. *** marks $P < 0.001$, ** marks $P < 0.01$, * marks $P < 0.05$.

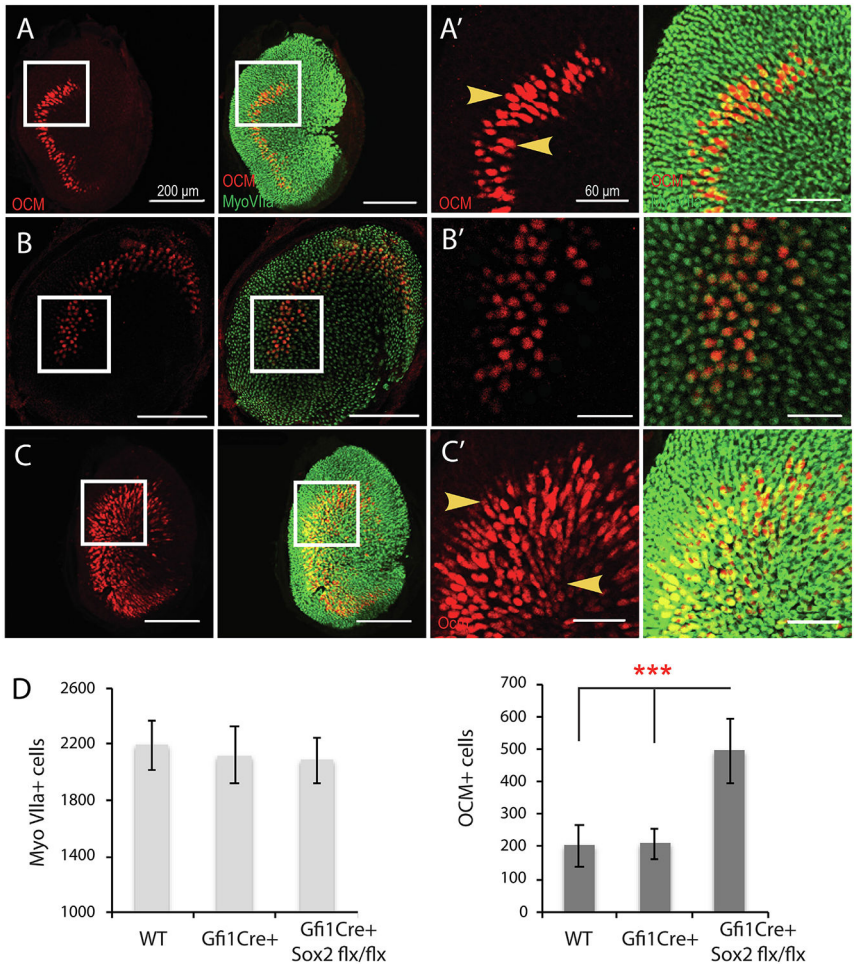

Fig. 6.

The number of Type I HCs increased in striola at P5. (A and A′) In the utricle, Type I HCs expressed oncomodulin in the striolar region. (B and B′) *Gfi-1-Cre+* mice did not increase the number of oncomodulin+ Type I HCs but expanded the striolar region in the P5 utricle. C and C′ *Sox2* knockout in HCs increased the number of oncomodulin+ Type I hair cells and expanded the striolar region in P5 *Gfi-1-Cre*; $Sox2^{flox}$ mice. D The total number of Type I HCs (oncomodulin+) increased in *Sox2* knockout mice. There were significant differences between *Sox2* knockout mice and the other two groups ($F(2,21) = 35.357$, $P < 0.001$). There was no significant differences in the total number of HCs (myosin VIIa+) among the three groups ($F(2,21) = 0.792$, $P = 0.468$). Arrows point to the area of oncomodulin+/MyoVIIa+ cells. Values and error bars represent the means ± SD. SOX2, SRY-box 2; HC, hair cell; *Gfi1*, growth factor independent 1 transcriptional repressor; *Cre*, causes recombination. *** marks $P < 0.001$, ** marks $P < 0.01$, * marks $P < 0.05$.

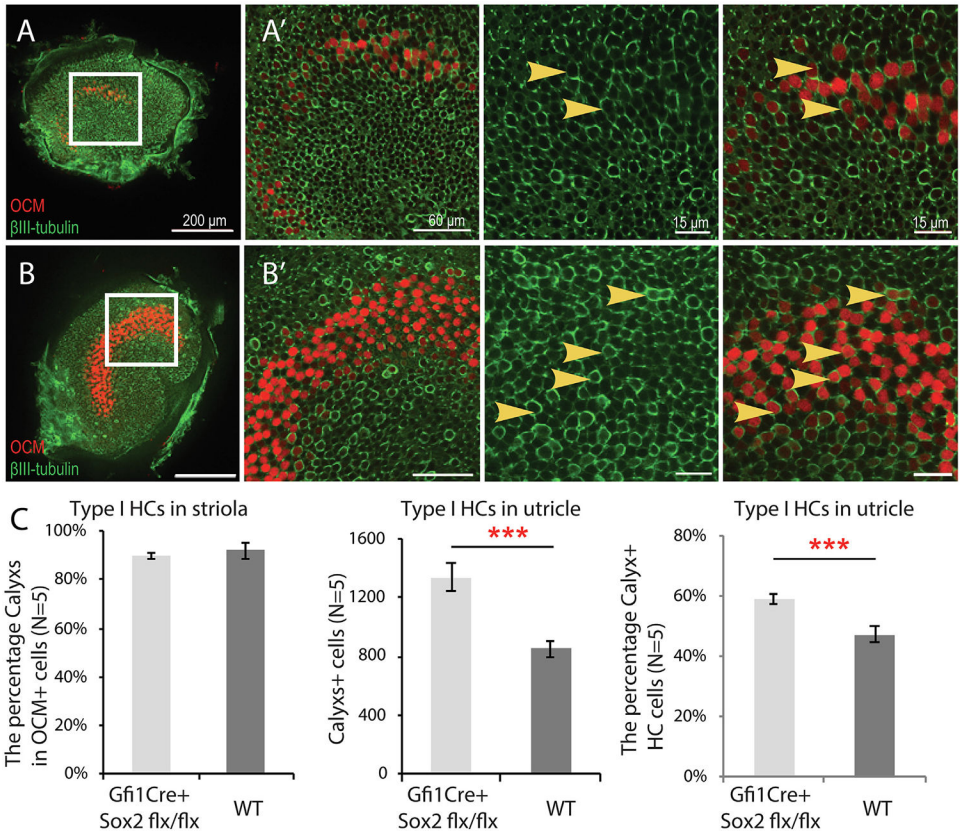

Fig. 7.

Sox2 knockout increased the number of calyces at P5. Type I HCs have characteristic calyces, visualized by β-tubulin III staining. Type I HCs in the striola also express oncomodulin. (A) Oncomodulin+ cells outlined in the striolar region. β-tubulin III+ calyces were observed in the striolar and extrastriolar regions in the wild-type utricle. (A′) High magnification images showed that Type I HCs were enclosed with β-tubulin III+ calyces. (B) More oncomodulin+ cells were observed in the *Gfi-1-Cre*; $Sox2^{flox}$ mutant. Oncomodulin+ cells had β-tubulin III+ calyces. (B′) High magnification images of B. (C) Quantification of *Sox2* knockout mutants and wild-type utricles. 92% and 89.9% of the oncomodulin+ cells had calyces in the wild-type and mutant utricles ($t(8) = 1.398$, $P = 0.219$). The number of Type I HCs was calculated as the β-tubulin III+ calyces per total MYO7A+ HCs ($t(8) = 10.153$, $P < 0.001$). The percentage of Type I HCs increased from 47.3% in the wild-type to 59.1% in the *Sox2* mutants ($t(8) = 9.057$, $P < 0.001$). Arrows point to oncomodulin+ and β-tubulin III+ cells. Values and error bars represent the means ± SD. SOX2, SRY-box 2; HC, hair cell; *Gfi1*, growth factor independent 1 transcriptional repressor; *Cre*, causes recombination. *** marks $P < 0.001$, ** marks $P < 0.01$, * marks $P < 0.05$.

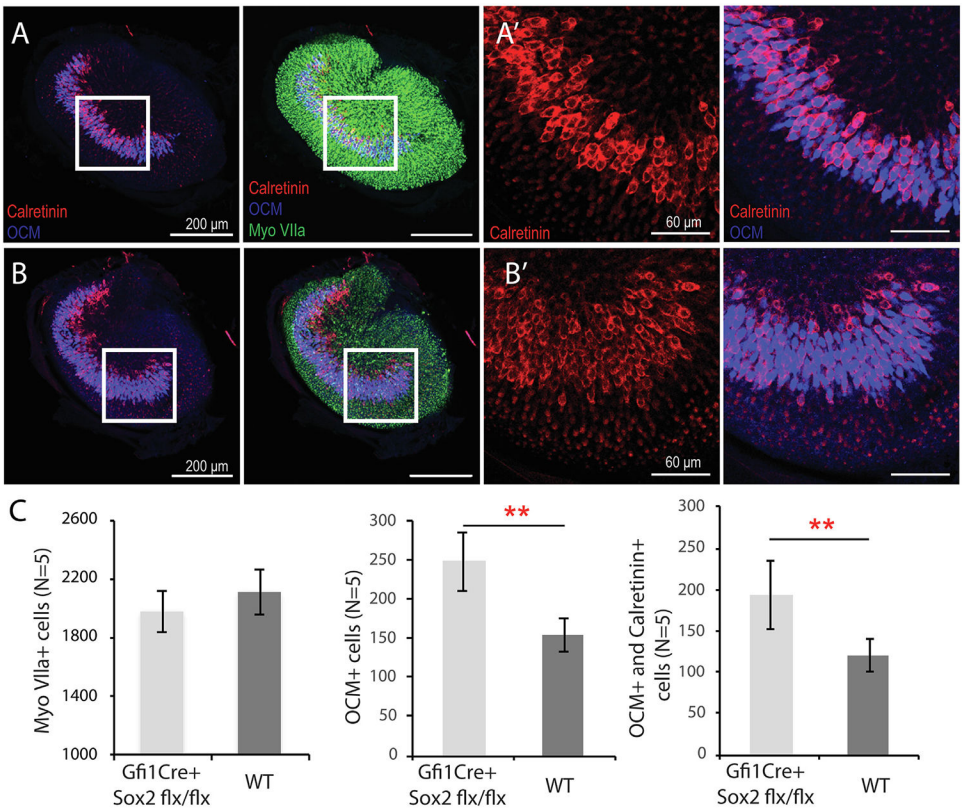

Fig. 8.

Increased number of Type I HCs in the striola was maintained in the adult utricle. (A and A′) Oncomodulin+ Type I HCs were enclosed by calretinin+ calyces in the striolar region. (B and B′) At P60, the striolar region in *Gfi-1-Cre*; *Sox2*^{flox} mice was larger and had more oncomodulin+ and calretinin+ cells. C The total number of HCs (MyoVIIa+) was unchanged ($t(8) = 1.500$, $P = 0.168$). Quantification revealed that utricles of *Sox2* knockout mice had 160.3% OCM Type I HCs ($U(5,5) = 0$, $P = 0.004$) (© mid) and 161.2 *%* calyces ($t(8) = 3.57$, $P = 0.007$) as compared with wild-type mice. Arrows point to oncomodulin+ cells and calretinin+ calyces. Values and error bars represent the means ± SD. SOX2, SRY-box 2; HC, hair cell; *Gfi1*, growth factor independent 1 transcriptional repressor; *Cre*, causes recombination. *** marks $P < 0.001$, ** marks $P < 0.01$, * marks $P < 0.05$.

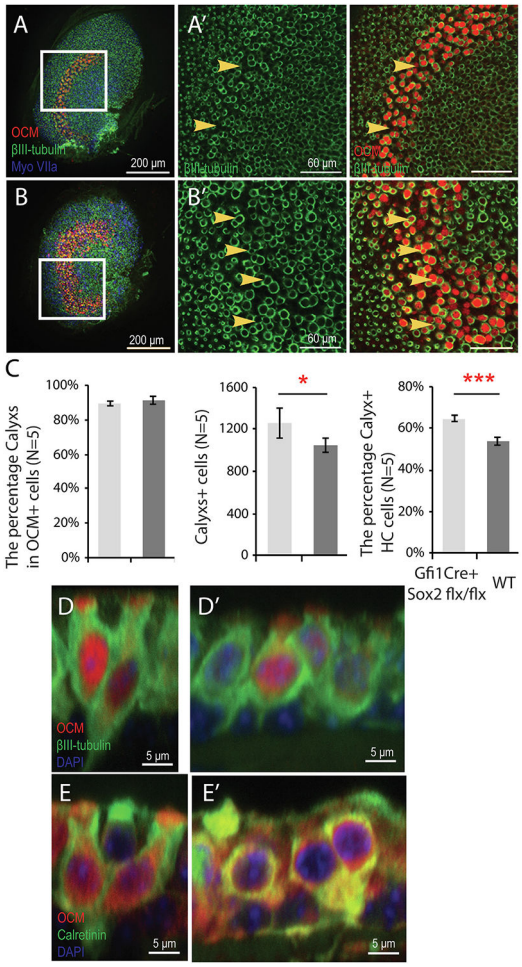

Fig. 9.

Sox2 knockout increased the number of calyx+ Type I HCs in adult mice. Calyces around the Type I HC are visualized by β-tubulin III staining in both the striola and extrastriola. Type I HCs in the striola also express oncomodulin. (A) Oncomodulin+ and β-tubulin III+ calyces in the wild-type utricle. (B) More oncomodulin+ cells were observed in the *Gfi-1-Cre*; *Sox2*^{flox} mutant. Most oncomodulin+ cells had β-tubulin III+ calyces. (C) Quantification of Type I HCs in *Sox2* knockout mutant and wild-type utricles. 91.5% and 89.3% of the oncomodulin+ cells had calyces in wild-type and mutant utricles ($t(8) = 2.041$, $P = 0.076$). The total number of cells with a calyx in the *Sox2* mutant was 119% of that in the wild-type utricle ($t(8) = 2.893$, $P = 0.02$). The percentage of Type I hair cells increased from 53.6% in the wild-type to 64.3% in the *Sox2* mutants ($t(8) = 8.451$, $P < 0.001$). The Type I percentage was calculated as the number of β-tubulin III+ calyces relative to the total myosin VIIa+ hair cells. (D and D′) High-magnification images from XZ image stacks showed that Type I HCs were enclosed by β-III-tubulin positive calyces in the striolar region of a wild-type utricle and *Sox2* knockout mutants. (E and E′), Calretinin+ calyces in the striolar region of a wild-type utricle and *Gfi-1-Cre*; *Sox2*^{flox} mutant. Arrows point to oncomodulin+ and β-tubulin III+ cells. Values and error bars represent the means ± SD. SOX2, SRY-box 2; HC, hair cell; *Gfi1*, growth factor independent 1 transcriptional

repressor; *Cre*, causes recombination. *** marks $P < 0.001$, ** marks $P < 0.01$, * marks $P < 0.05$.